EMERALD

ElectroMagnetic imaging for a novel genERation of medicAL Devices

Performance assessment of microwave tomography and radar imaging using an anthropomorphic brain phantom

Olympia Karadima, Navid Ghavami, Ioannis Sotiriou, Panos Kosmas

King's College London, London, UK

Funded by:

EPSRC Engineering and Physical Sciences Research Council and

This project has received funding from the European Union's Horizon 2020 research and innovation programme under grant agreement No **764479**

URSI GASS 2020

Motivation

Current imaging techniques (MRI, CT scans)
- Expensive
- Time consuming

Microwave imaging (MWI)
- Quick, safe and bed-side diagnosis
- User friendly design
- Cost effective

Applications in medical imaging devices
- Breast cancer detection
- **Differentiation and detection of brain stroke**

Microwave tomography

Estimation of the spatial distribution of dielectric properties in a region of interest by solving an electromagnetic inverse scattering problem

Radar imaging

Finds the solution to a simpler problem of discovering the scattering map based on contrast amongst the dielectric properties

Outline

- Background and problem statement
- Related work
- Methodology
- Experimental configuration
- Results
- Conclusions and future work

Background and problem statement

Strong and robust imaging algorithms

DBIM-TwIST tomography algorithm[1]

- Permits accurate reconstruction of phantom's internal dielectric properties
- Can distinguish between h- and i-strokes

Huygens based radar algorithm [2]

- Does not require matrix generation and inversion
- Its application is not limited to certain known geometries
- It has shown promising results in previous research on breast and skin cancer detection

Hardware characteristics

- Increase the penetration depth into the lossy tissues
- Secure adequate spatial resolution images

↑

Antennas operating below 2 GHz

Experiment characteristics

- Multi-layer anthropomorphic model of the head

↑

Gel-based head phantom

KING'S College LONDON
University of London

Related work

Multiple prototypes for h-stroke detection exist, but no MWT prototypes for differentiation between h-stroke and i-stroke in a wide frequency range.[1-7]

Challenges:

- High heterogeneity of the human body[8]
- Non-linear solution[9] ⟶ **DBIM-TwIST**[1]
- Non-unique solution[9]

Optimal characteristics for a MWT prototype:

- Number of antennas: 24[10]
- Optimal frequency range: 0.6–1.5 GHz[11]
- Matching medium permittivity:10-40[11]

Reconstructed real part of the complex permittivity for h-stroke, 25% i-stroke and 50% i-stroke[12]

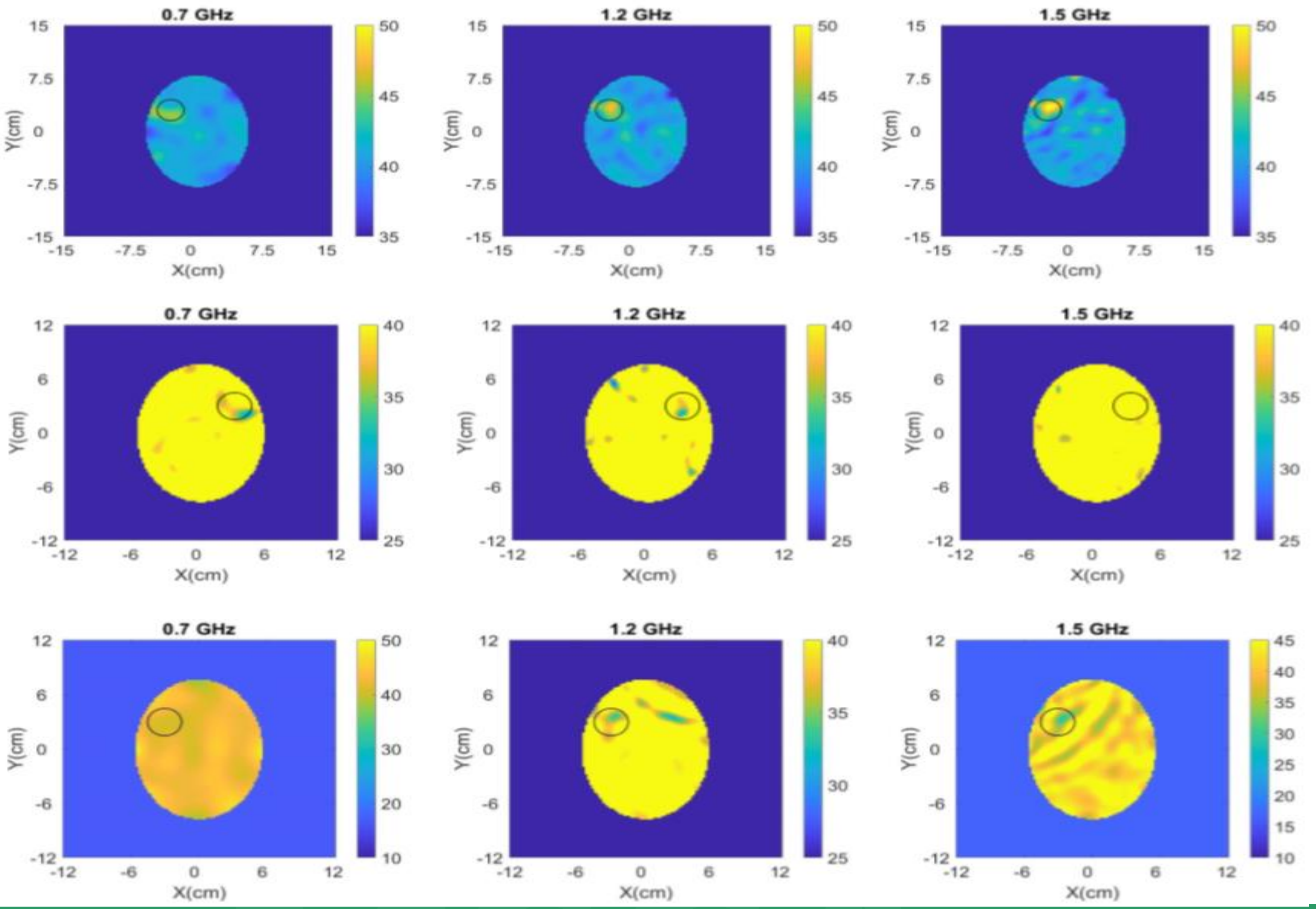

Methodology

DBIM-TwIST algorithm

DBIM iterative approach

1. Approximating the non-linear integral equation via the Born approximation at each iteration

$$\begin{aligned}\boldsymbol{E_s}(\boldsymbol{r_n},\boldsymbol{r_m}) &= \boldsymbol{E}(\boldsymbol{r_n},\boldsymbol{r_m}) - \boldsymbol{E_b}(\boldsymbol{r_n},\boldsymbol{r_m}) \\ &= \omega^2\mu\int_V \boldsymbol{G_b}(\boldsymbol{r_n},\boldsymbol{r})\boldsymbol{E_b}(\boldsymbol{r},\boldsymbol{r_m})(\epsilon(\boldsymbol{r}) - \epsilon_b(\boldsymbol{r})d\boldsymbol{r})\end{aligned}$$

2. Estimated Green's function for the background medium

$$G_b(\boldsymbol{r}_n,\boldsymbol{r}) = \frac{i}{\omega\mu}E_b(\boldsymbol{r},\boldsymbol{r}_n)$$

3. Discretize integral equation

$$E_s(\boldsymbol{r}_n,\boldsymbol{r}_m) \approx i\omega\int_V E_b(\boldsymbol{r},\boldsymbol{r}_m)E_b(\boldsymbol{r},\boldsymbol{r}_n)O(\boldsymbol{r})d\boldsymbol{r}$$

$$\boldsymbol{b}(\omega) = \boldsymbol{A}(\omega)\boldsymbol{o}$$

4. Solve the non-linear problem iteratively and update background properties

$$\epsilon_{bi+1} = \epsilon_{bi} + \hat{\boldsymbol{o}}_{i+1}$$

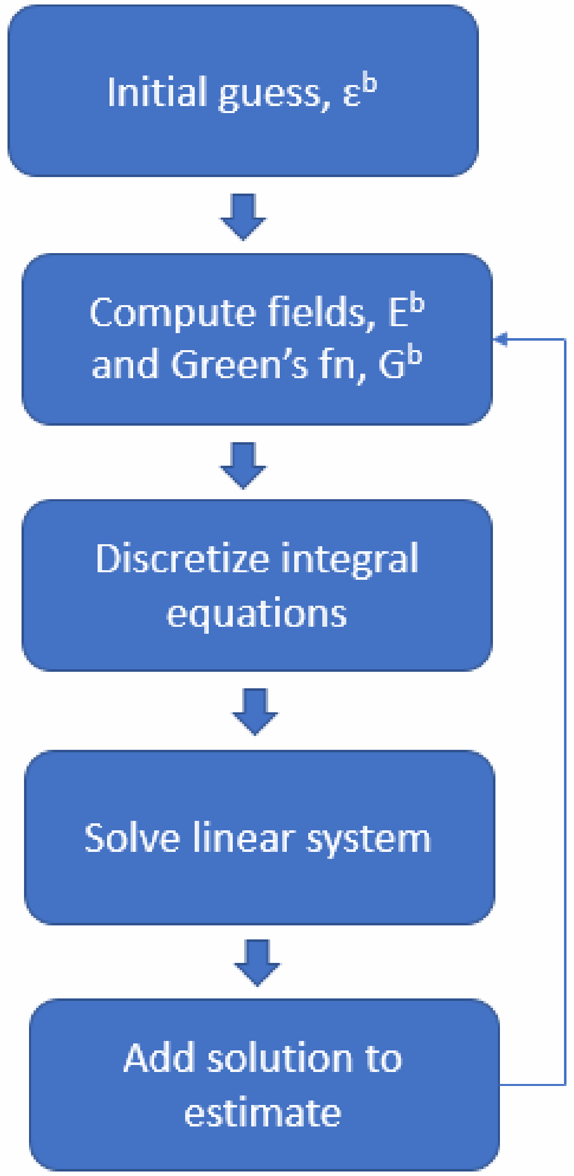

DBIM-TwIST algorithm

Solves the linear problem at each DBIM iteration as a linear inverse problem.
Splitting of the matrix in a two step iterative equation:

$$\begin{aligned}\boldsymbol{x}_{t+1} &= (1-\alpha)\boldsymbol{x}_{t-1} + (\alpha-\beta)\boldsymbol{x}_t + \beta\Gamma_\lambda(\boldsymbol{x}_t) \\ \Gamma_\lambda(\boldsymbol{x}) &= \Psi_\lambda(\boldsymbol{x} + A^T(\boldsymbol{y} - A\boldsymbol{x}))\end{aligned}$$

Next solution depends the current solution as well as previous solution.

Methodology

Huygens based radar algorithm

Let us consider an object in free space:

- the external cylinder is characterized by a low dielectric constant
- the internal cylinder is characterized by a higher dielectric constant

Goal: Identifying the presence and location of the inclusion by using only the field E_{nm} measured outside the cylinder

The field inside the cylinder is reconstructed using superimposition of the fields radiated by the *N* observation points:

$$E_{\mathrm{HP}}(\rho, m, f) = \sum_{n=1}^{N} E_{nm}(f) G(k|\rho_n - \rho|)$$

Resulting normalized intensity calculated through summing contributions from all receiving positions (*m*) and all frequency points (*l*):

$$I_{\mathrm{HP}}(\rho) = \sum_{m=1}^{M} \left[\sum_{l=1}^{L} E_{\mathrm{HP}}(\rho, m, f_l) \right]^2$$

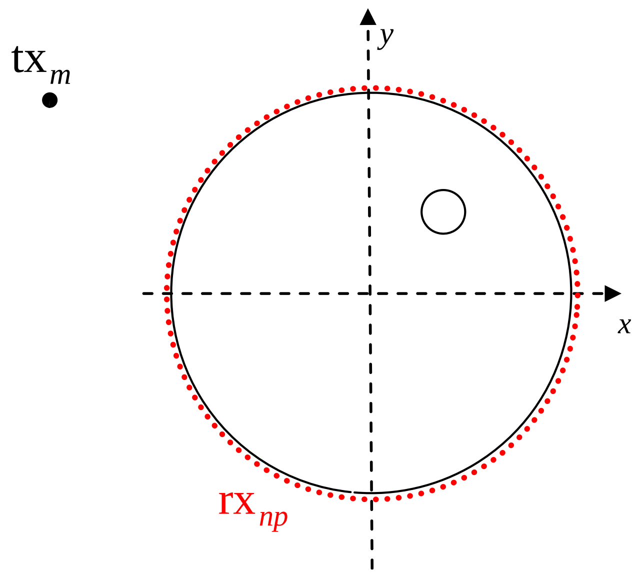

Inverse Problem

Methodology

Experimental configuration

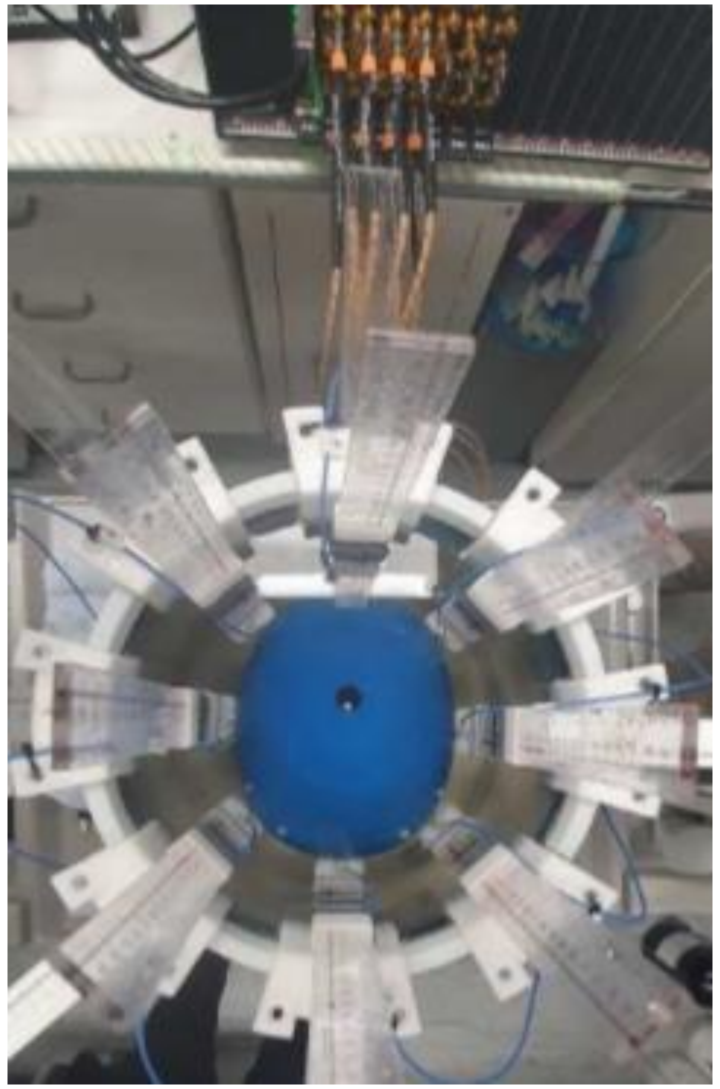

Tomography setup
8-transceiver array

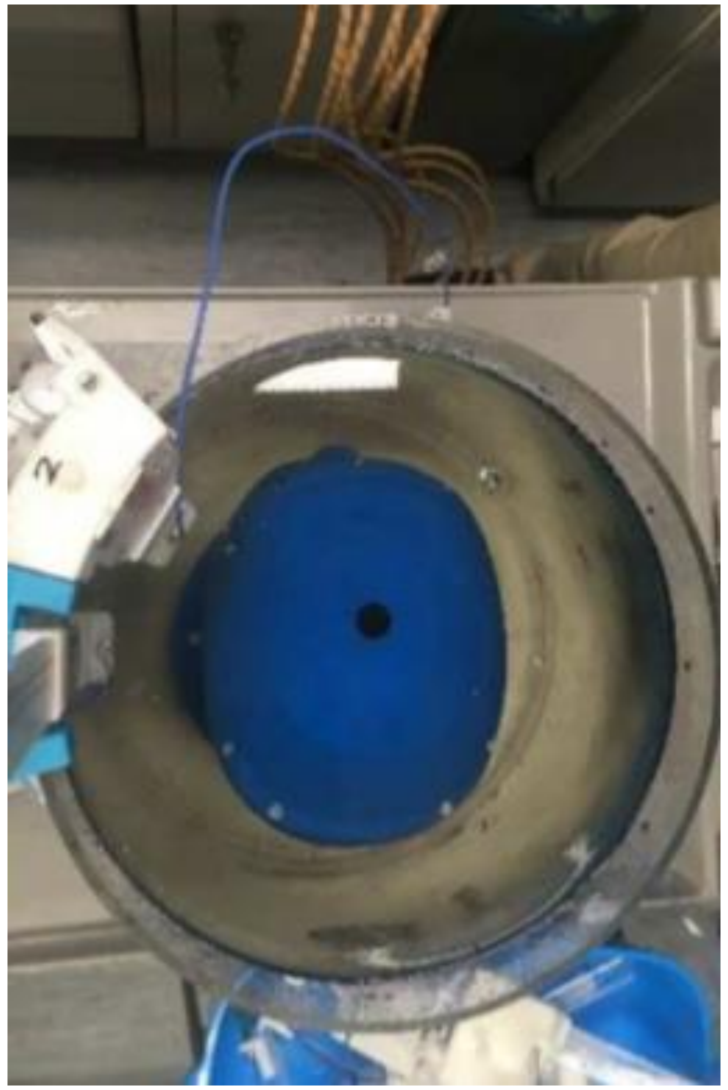

Radar setup
2 rotating antennas
acting as Tx and Rx

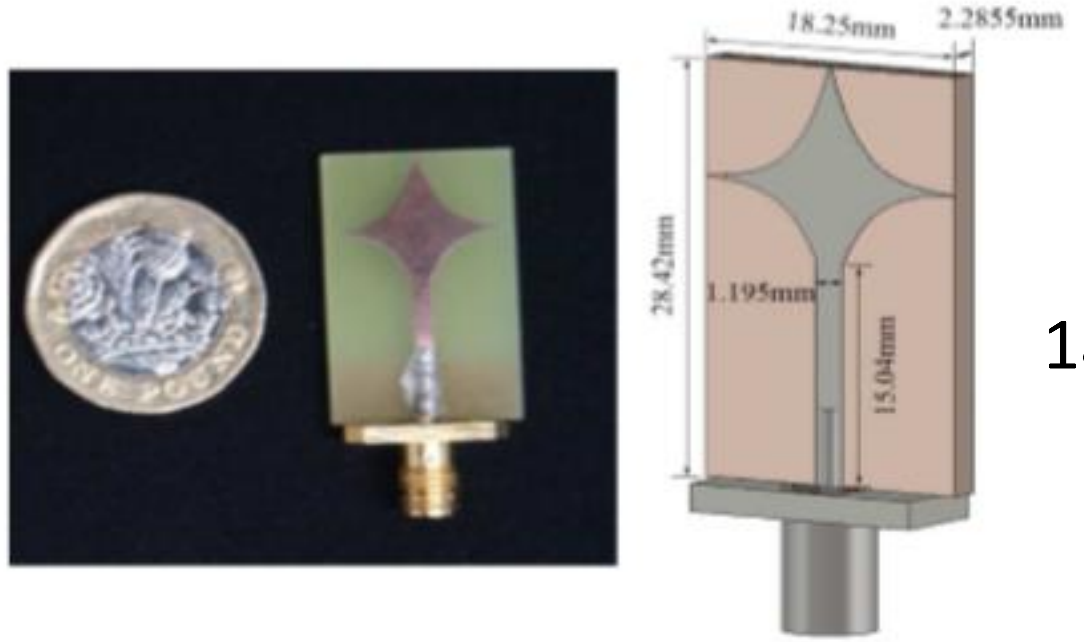

Spear antenna
18.25 mm by 28.42 mm FR-4

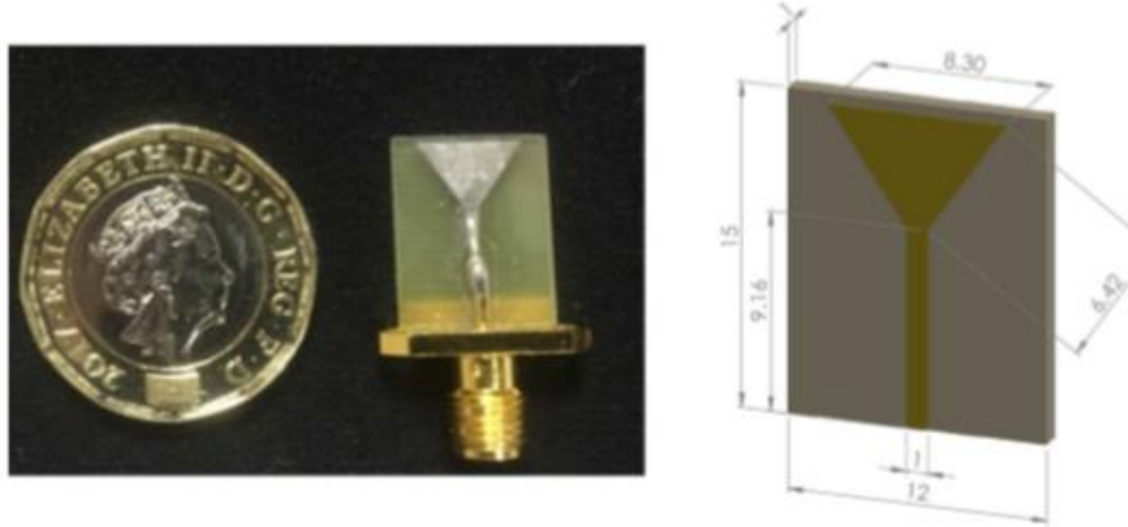

Triangular antenna
12 mm by 15 mm FR-4

KING'S College LONDON
University of London

Methodology

Experimental configuration

Concentrations of materials of human tissue mimicking phantoms

100 ml phantoms	Water	Gelatine powder	Kerosene	Oil	Propanol	Surfactant
Brain	60 ml	11 gr	13 ml	13 ml	2.5 ml	1.5 ml
Blood/CSF	80 ml	16 gr	-	-	3 ml	1 ml

Dielectric properties of tissue mimicking phantoms at 1 GHz

	ε′	ε′′
Brain	41.1	0.35
Blood/CSF	62.3	0.56ε′

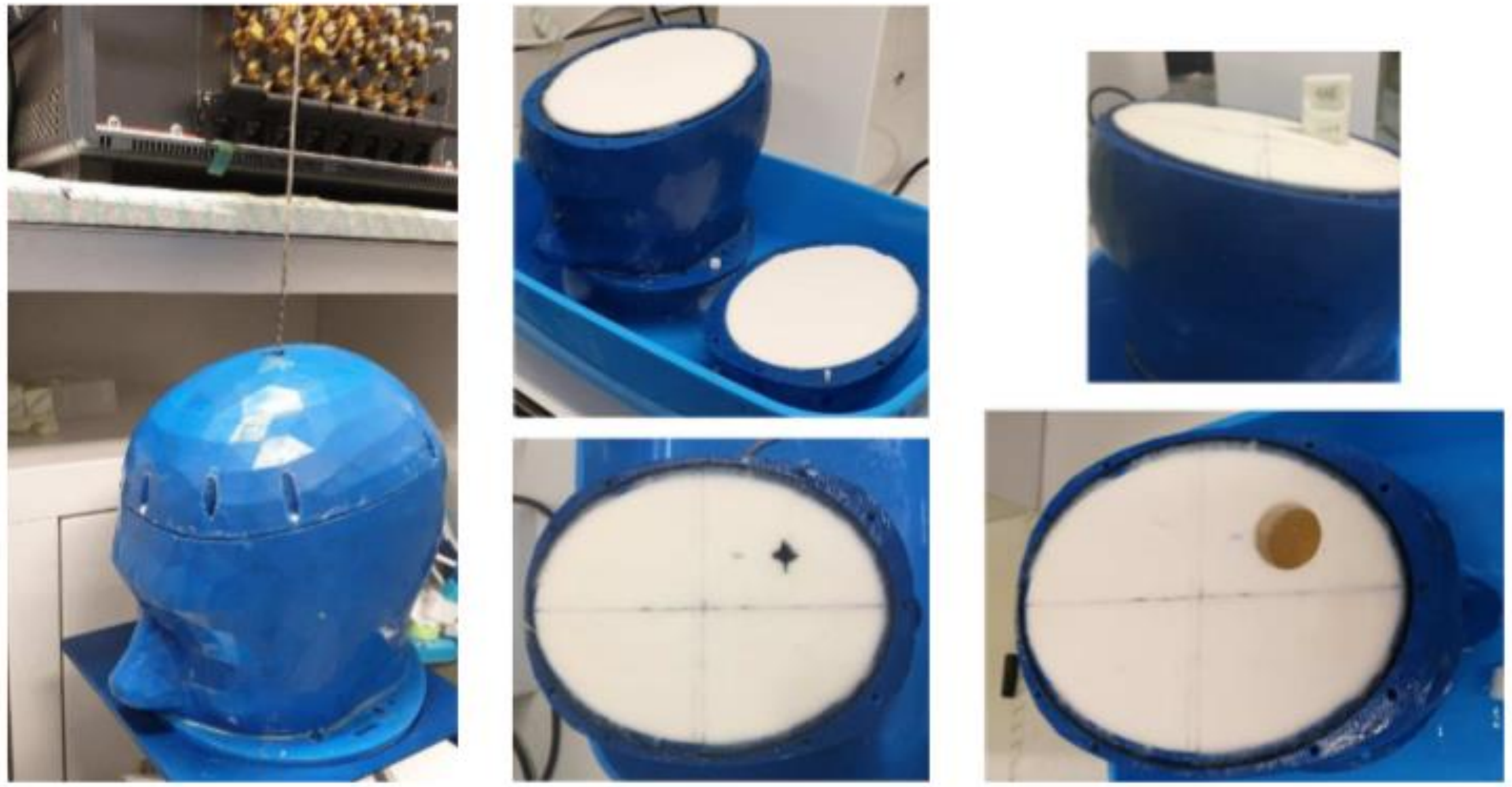

Anthropomorphic head model and the preparation stages

King's College London University of London

Experimental Results

DBIM-TwIST results

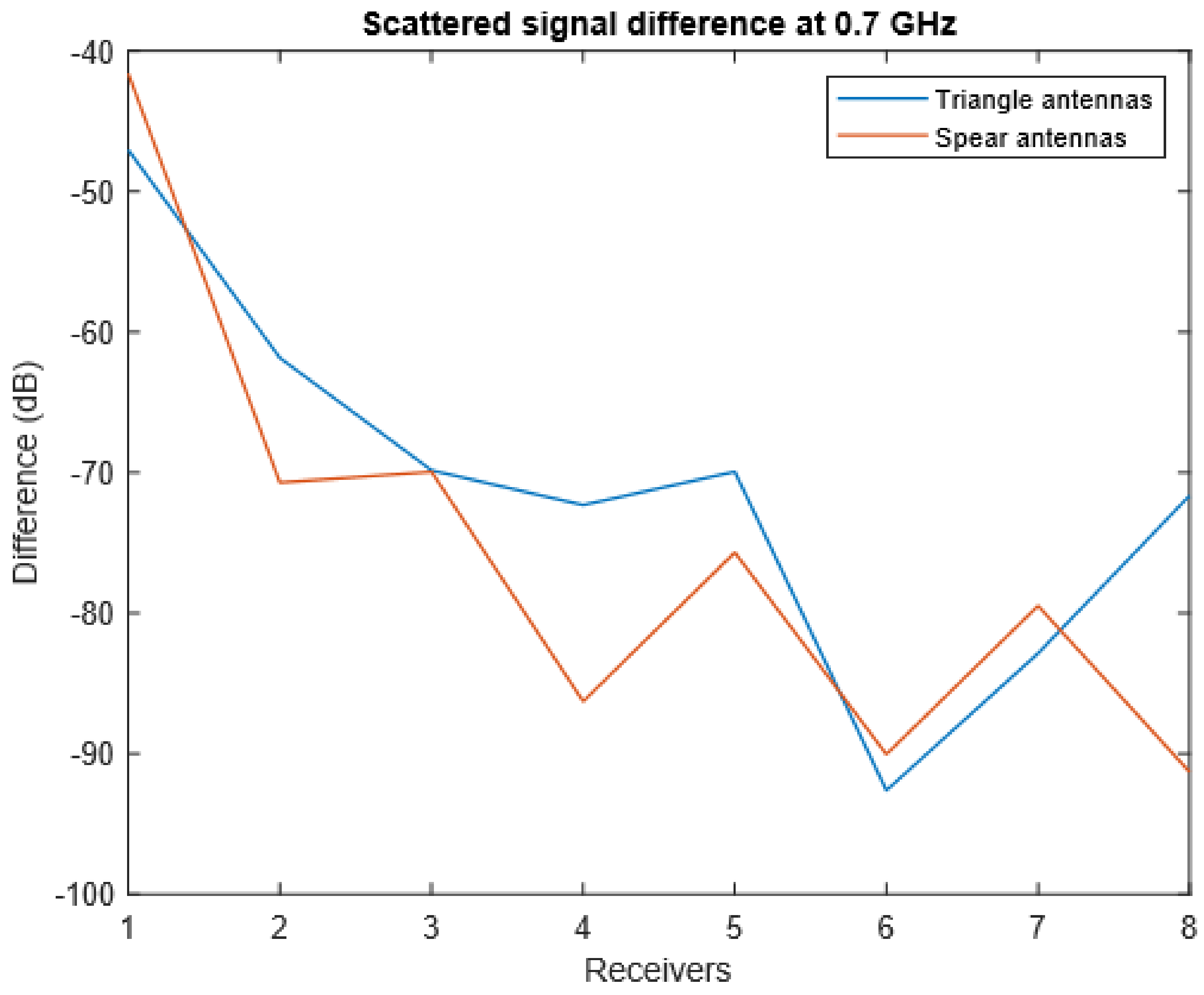

Reconstructed ε' using trianglular antennas

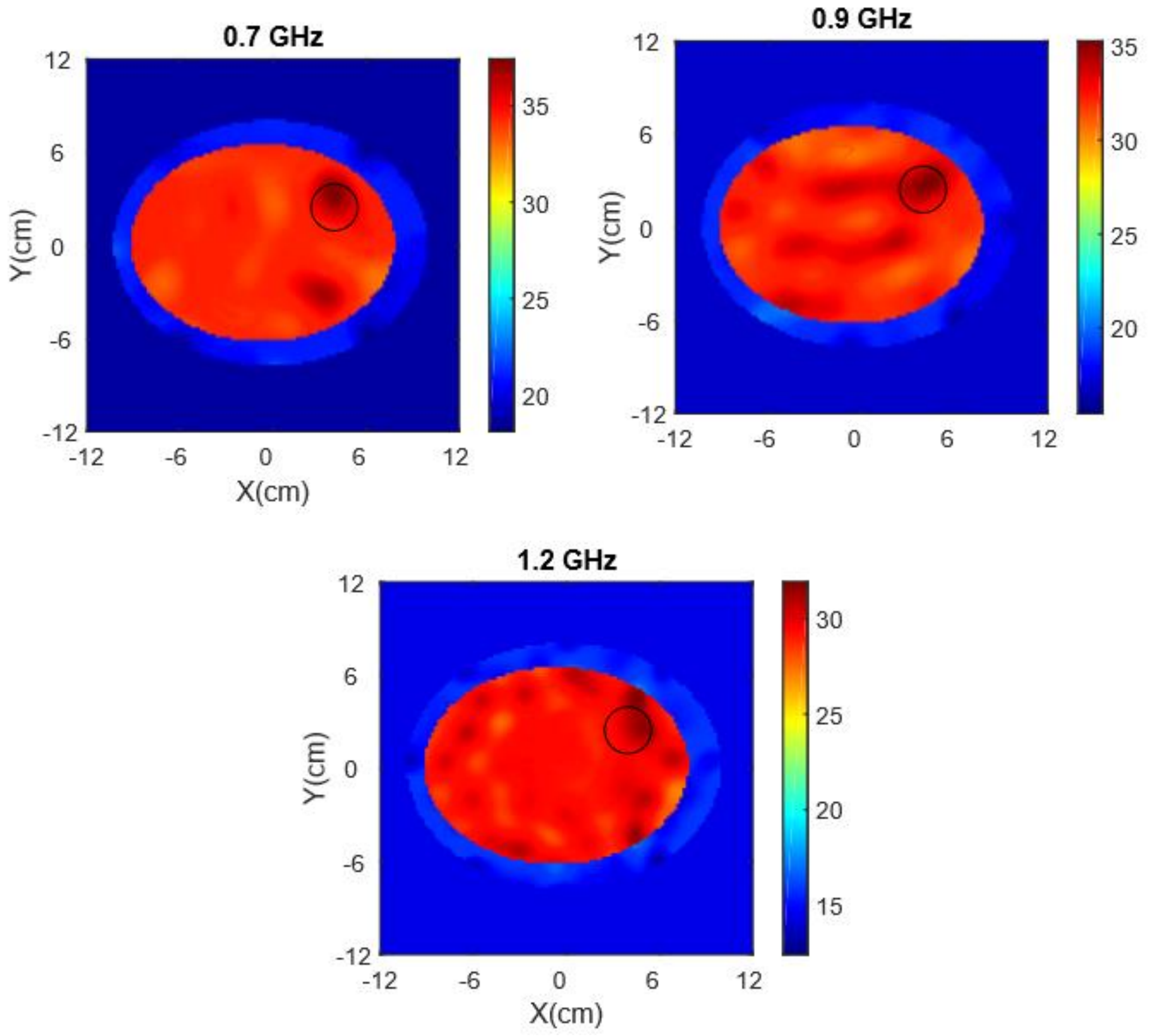

Experimental Results

Huygens based radar results

S-parameter magnitude (dB) plot for different antenna distances

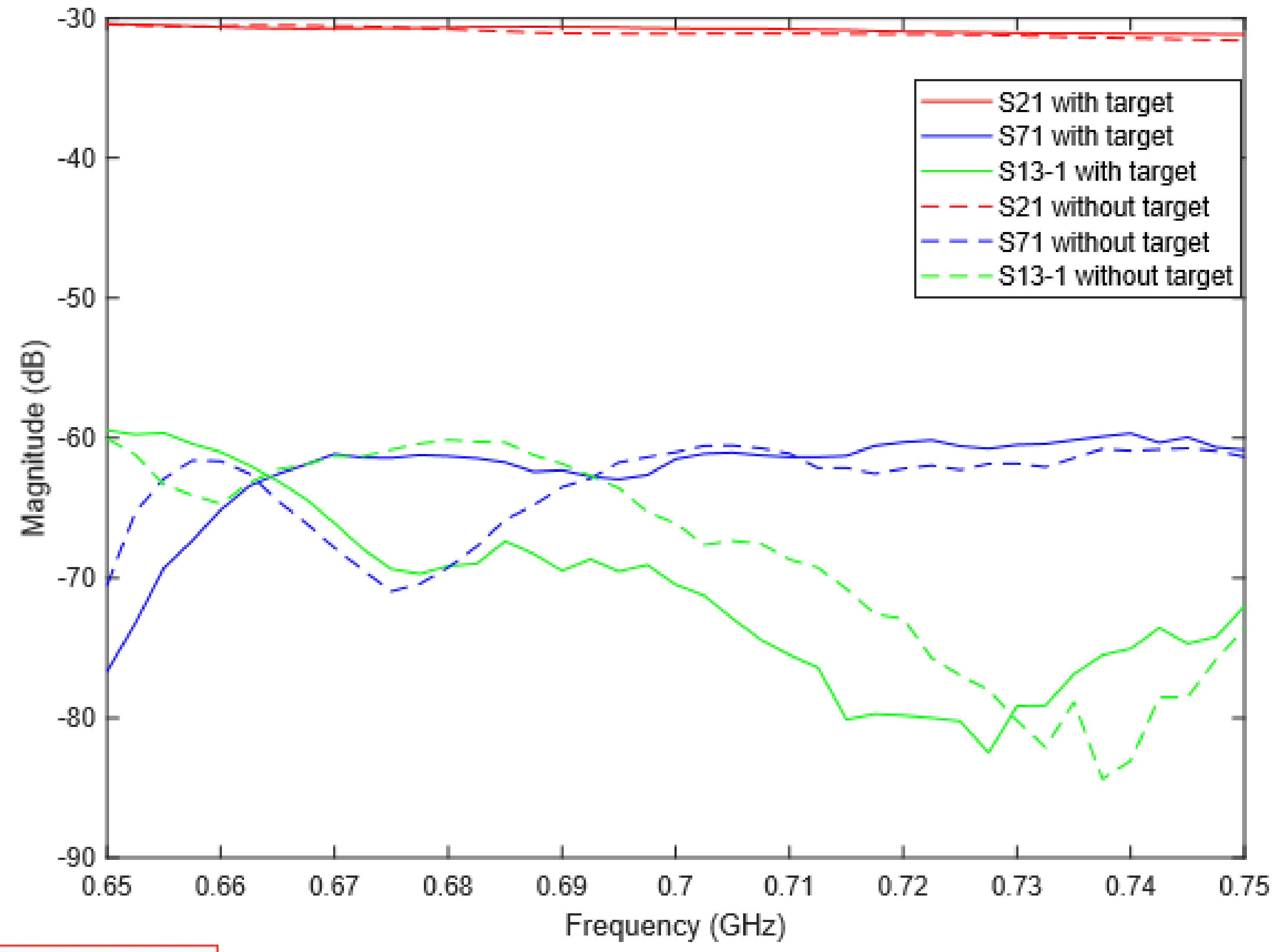

Intensity images of the phantom before and after image adjusting

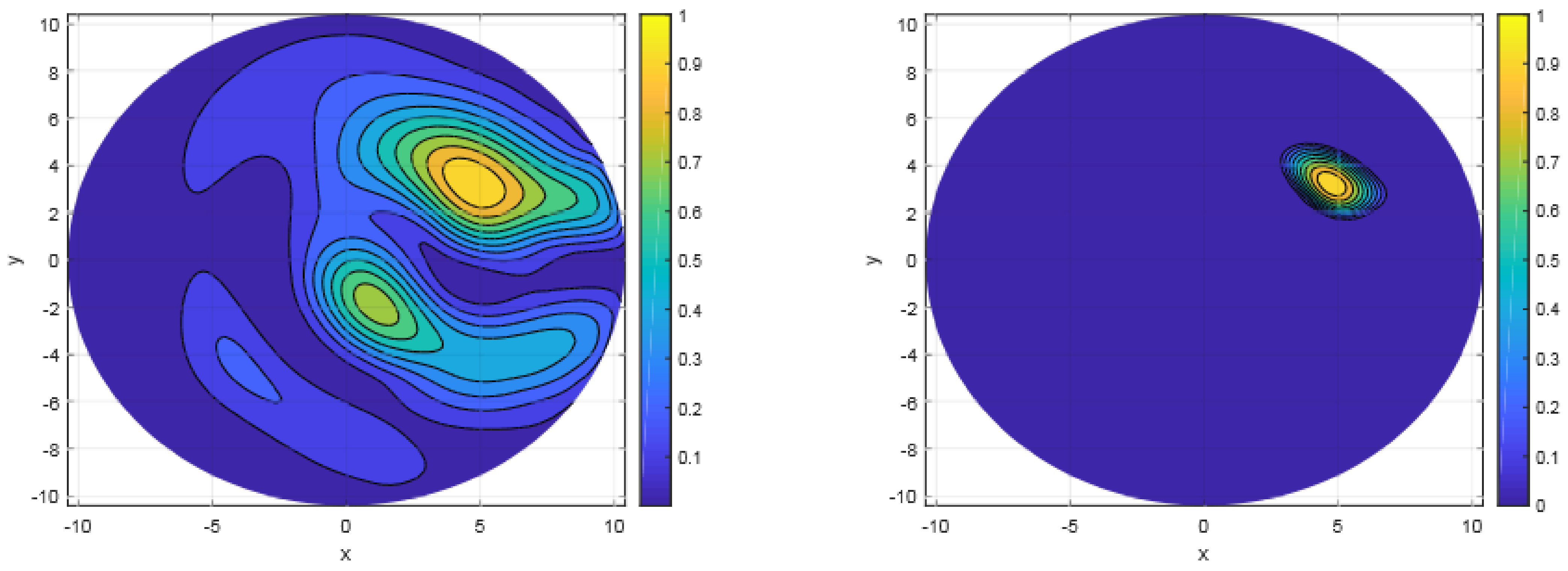

(axis are in cm)

Conclusions and future work

Conclusions:

1. Target can be located through subtraction between “with-target” and “without-target” phantoms.
2. Both algorithms are capable of detecting and localizing the blood mimicking target in its approximate position.
3. Triangular antennas perform better with tomography while spear antennas produce better images with radar imaging .

Future work:

1. Increasing complexity and inhomogeneity of the head models for more realistic representation.
2. Development of a hybrid image processing algorithm, combining the strongest features of both DBIM-TwIST and Huygens methods.

References

[1] Z. Miao and P. Kosmas, “Multiple-frequency dbim-twist algorithm for microwave breast imaging,” IEEE Transactions on Antennas and Propagation, vol. 65, no. 5, pp. 2507–2516, 2017.
[2] N. Ghavami, G. Tiberi, D.J. Edwards, A. Monorchio, “UWB Microwave Imaging of Objects With Canonical Shape”, IEEE Transactions on Antennas and Propagation, Vol. 60 , Issue: 1, 2012 , pp. 231-239.
[3] M. Persson, A. Fhager, H. D. Trefná, Y. Yu, T. McKelvey, G. Pegenius, J.-E. Karlsson, and M. Elam, “Microwave-based stroke diagnosis making global prehospital thrombolytic treatment possible,” IEEE Transactions on Biomedical Engineering, vol. 61, no. 11, pp. 2806–2817, 2014.
[4] J. A. Tobon Vasquez, R. Scapaticci, G. Turvani, G. Bellizzi, N. Joachimowicz, B. Duchêne, E. Tedeschi, M. R. Casu, L. Crocco, and F. Vipiana, “Design and experimental assessment of a 2d microwave imaging system for brain stroke monitoring,” International Journal of Antennas and Propagation, vol. 2019, 2019.
[5] A. T. Mobashsher, K. Bialkowski, A. Abbosh, and S. Crozier, “Design and experimental evaluation of a non-invasive microwave head imaging system for intracranial haemorrhage detection,” Plos one, vol. 11, no. 4, p. e0152351, 2016.
[6] I. Merunka, A. Massa, D. Vrba, O. Fiser, M. Salucci, and J. Vrba, “Microwave tomography system for methodical testing of human brain stroke detection approaches,” International Journal of Antennas and Propagation, vol. 2019, 2019.
[7] M. Hopfer, R. Planas, A. Hamidipour, T. Henriksson, and S. Semenov, “Electromagnetic tomography for detection, differentiation, and monitoring of brain stroke: A virtual data and human head phantom study.,” IEEE Antennas and Propagation Magazine, vol. 59, no. 5, pp. 86–97, 2017.
[8] V. Zhurbenko, “Challenges in the design of microwave imaging systems for breast cancer detection,” Advances in Electrical and Computer Engineering, vol. 11, no. 1, pp. 91–96, 2011.

References

[9] G. N. Bindu, S. J. Abraham, A. Lonappan, V. Thomas, C. K. Aanandan, and K. Mathew, “Active microwave imaging for breast cancer detection,” Progress In Electromagnetics Research, vol. 58, pp. 149–169, 2006.
2007.

[10] R. Scapaticci, J. Tobon, G. Bellizzi, F. Vipiana, and L. Crocco, “Design and numerical characterization of a low-complexity microwave device for brain stroke monitoring,” IEEE Transactions on Antennas and Propagation, vol. 66, no. 12, pp. 7328–7338, 2018.

[11] R. Scapaticci, L. Di Donato, I. Catapano, and L. Crocco, “A feasibility study on microwave imaging for brain stroke monitoring,” Progress In Electromagnetics Research, vol. 40, pp. 305–324, 2012.

[12] O. Karadima, M. Rahman, I. Sotiriou, N. Ghavami, P. Lu, S. Ahsan and P. Kosmas, “Experimental Validation of Microwave Tomography with the DBIM-TwIST Algorithm for Brain Stroke Detection and Classification,” Sensors, vol. 20, 2020.